IAC-12.C1.1.11
SOLAR SAIL STATION KEEPING OF HIGH-AMPLITUDE VERTICAL LYAPUNOV ORBITS IN THE SUN-EARTH SYSTEM

Ariadna Farrés
Math. Institute, Bourgogne Univ. & CNRS, France, ariadna.farres@u-bourgogne.fr
Matteo Ceriotti
University of Glasgow, United Kingdom, matteo.ceriotti@glasgow.ac.uk

Abstract

This paper studies the stability and controllability of a solar sail on displaced, high-amplitude vertical Lyapunov orbits in the Sun-Earth system. In previous works, it was found that these orbits could be used for quasi-continuous coverage of the poles of the Earth. However, these orbits are unstable and an active control is required to remain close to them. Here we describe the types of instabilities for various orbits in the vertical Lyapunov family, and then propose two different station-keeping strategies. One based on a linear quadratic regulator, and the other on the Floquet multipliers. We have selected three orbits, with different characteristics, for this study. It results that both methods manage control the solar sail, in the vicinity of the nominal orbits, and a comparison of the control requirements and performances is presented.

I. INTRODUCTION

The recent successful deployment of the sail performed by JAXA's IKAROS mission[1] has finally validated the concept of solar sailing for spacecraft propulsion. A solar sail, by reflecting the photons from the Sun, offers the potential capability of delivering a continuous thrust without the need of any propellant mass, and therefore for a potentially unlimited amount of time.[2]

This capability is extremely interesting for long interplanetary transfers, but also opens up the way to missions requiring the spacecraft to be in a displaced or artificial equilibrium point[3] or in a non-Keplerian orbit.[4] In both cases, a continuous acceleration is required to maintain the nominal orbit conditions.

Extensive work is found in the literature on a wide range of these Non-Keplerian orbits.[5,6] Recently it was proposed the use of solar sails on large-amplitude eight-shaped vertical Lyapunov orbits at Lagrangian points L_1 and L_2 of the Sun-Earth system.[7] These orbits naturally bend towards the Earth for a range of amplitudes, and it was shown that the use of a solar sail of modest lightness number displaces these orbits further towards the Earth. Therefore, they constitute a viable way to continuously cover the high-latitude regions and the poles of the Earth, for polar weather forecast, ice pack monitoring and ship routing. However, it was also shown that these orbits are highly unstable, and therefore a robust and reliable control strategy is essential to exploit these orbits in a real mission scenarios, where even small perturbations can potentially have extreme consequences.

In this paper we want to study the controllability of these kind of orbits. In Section III. we will briefly describe the vertical family of Lyapunov orbits around L_2 and their main stability properties. In Section IV. we propose two different station keeping strategies to control the instability of these orbits. One is based on a linear quadratic regulator (LQR)[8] and the other is based on the Floquet multipliers.[9] For both methods we will show how to derive a control loop such that a solar sail remains close to a reference orbit and test the two methods against three different orbits. It will be shown that these strategies manage to successfully control the trajectory of solar sail. Finally, we will compare the main differences between them.

II. EQUATIONS OF MOTION

To describe the dynamics of a solar sail in the Earth - Sun system we consider the Circular Restricted Three Body Problem (CRTBP) adding the Solar Radiation Pressure (SRP) due to the solar sail (CRTBPS). We assume that the Earth and Sun are point masses moving around their com-

mon centre of mass in a circular way, and that the solar sail is a massless particle that is affected by the gravitational attraction of both bodies and the SRP. We normalise the units of mass, distance and time, so that the total mass of the system is 1, the Earth - Sun distance is 1 and the period of its orbit is 2π. We use a synodic reference system with the origin at the centre of mass of the Earth - Sun system and such that the Earth and Sun are fixed on the x-axis (with its positive side pointing towards the Earth), the z-axis is perpendicular to the ecliptic plane and the y-axis completes an orthogonal positive oriented reference system (see Figure 1).

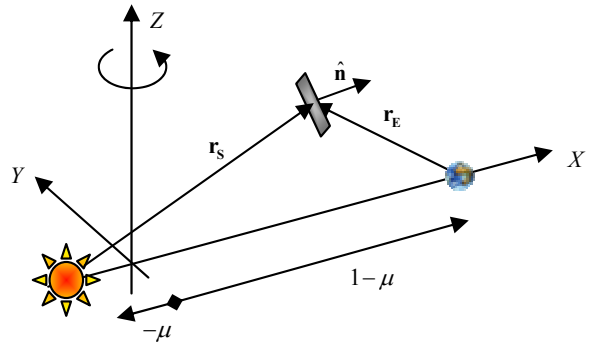

Fig. 1: Schematic representation of the position of the two primaries and the solar sail in the rotating reference system.

The acceleration given by the solar sail depends on its orientation and its efficiency. Here we consider the simplest model for a solar sail, we assume it to be flat and perfectly reflecting, so the acceleration due to the solar radiation pressure is in the normal direction to the surface of the sail.[2] Hence,

$$\mathbf{F_{sail}} = \beta \frac{1-\mu}{r_S^2} \langle \hat{\mathbf{r}}_\mathbf{S}, \hat{\mathbf{n}} \rangle^2 \hat{\mathbf{n}},$$

where $\mathbf{r_S}$ is the Sun - spacecraft vector, $\hat{\mathbf{r}}_\mathbf{S} = \mathbf{r_S}/r_S$ and $\hat{\mathbf{n}}$ is the normal direction to the surface of the sail (unit vector).

For a more realistic model one should account for the absorption of the photons by the surface of the sail. In this case, an extra component in the transverse direction of the sail must be added slightly changing the efficiency of the sail and the direction of the acceleration vector.[2]

Within our assumptions, the equations of motion in the synodic reference system are:

$$\begin{aligned} \ddot{X} - 2\dot{Y} &= \frac{\partial \Omega}{\partial x} + \beta \frac{(1-\mu)}{r_S^2} \langle \hat{\mathbf{r}}_\mathbf{S}, \hat{\mathbf{n}} \rangle^2 n_X, \\ \ddot{Y} + 2\dot{X} &= \frac{\partial \Omega}{\partial y} + \beta \frac{(1-\mu)}{r_S^2} \langle \hat{\mathbf{r}}_\mathbf{S}, \hat{\mathbf{n}} \rangle^2 n_Y, \\ \ddot{Z} &= \frac{\partial \Omega}{\partial z} + \beta \frac{(1-\mu)}{r_S^2} \langle \hat{\mathbf{r}}_\mathbf{S}, \hat{\mathbf{n}} \rangle^2 n_Z, \end{aligned} \tag{1}$$

where $\Omega(X,Y,Z) = \frac{1}{2}(X^2 + Y^2) + \frac{1-\mu}{r_S} + \frac{\mu}{r_E}$. $r_S = \sqrt{(X+\mu)^2 + Y^2 + Z^2}$ and $r_E = \sqrt{(X-1+\mu)^2 + Y^2 + Z^2}$ are the Sun - sail and Earth - sail distances respectively; lastly, $\hat{\mathbf{n}} = (n_X, n_Y, n_Z)$.

III. VERTICAL LYAPUNOV FAMILY

It is a known fact that, when the effect of a solar sail is added to the CRTBP, families of "artificial" equilibrium points appear, replacing the five Lagrangian equilibrium points $L_{1,\ldots,5}$.[2] Moreover, some of these fixed points inherit the dynamics of the $L_{1,\ldots,5}$ and families of periodic orbits can be found for different fixed sail orientations.[6]

For the particular case $\hat{\mathbf{n}} = [1,0,0]$ the three collinear Lagrangian points $L_{1,2,3}$ are displaced towards the Sun due to the effect of the Solar radiation pressure. The linear dynamics around these three points is still centre $\times$ centre $\times$ saddle and two families of periodic, orbits each one related to one of the two oscillations given by the linear approximation. The orbits in these two families are know as the planar and vertical Lyapunov orbits. They present an interesting location and have already been used for different mission applications. A typical example are the well know Halo orbits around L_1 used for the SOHO mission.

In a recent work, Ceriotti and McInnes[7] proposed to use orbits in the L_2 vertical Lyapunov family for quasi-continuous polar observation. In fact, by choosing the appropriate initial condition and lightness number, it is possible to find a number of orbits in which the spacecraft hovers above one of the Earth's poles for a considerable fraction of its orbital period, and then, after crossing the ecliptic plane with high velocity, the spacecraft slows down to hover above the other pole. In that work, it was found that three spacecraft on the same orbit, phased 120 deg, are sufficient to offer continuous coverage of both the north and the south pole of the Earth.

All the orbits in the vertical Lyapunov family around the displaced $L_{1,2}$ are simultaneously symmetric with respect to the $\{Y = 0\}$ and $\{Z = 0\}$ planes and have an eight-

shape with two symmetric loops w.r.t. the $\{Z = 0\}$ plane. Using the different symmetries of the system, these families of periodic orbits can easily be found using a continuation scheme. All these orbits can be represented as fixed points on the Poincaré section $\Gamma = \{Y = 0, \dot{Y} > 0\}$. The initial condition for each of the periodic orbits on the Poincaré section is $[X_0, 0, Z_0, 0, V_{Y,0}, 0]^T$.

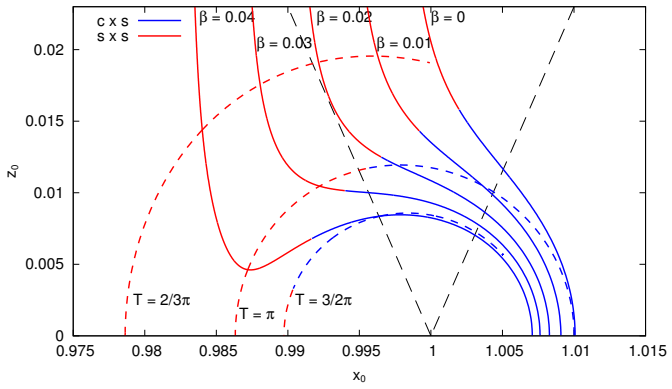

Fig. 2: Bifurcation diagram for the periodic orbits in the Vertical family around L_2. Continuous lines are orbits with a fixed β and the dashes lines are orbits with a fixed orbital period.

In Figure 2 we show the X, Z coordinates of different orbits in the vertical family on the Poincaré section, Γ. The points in the continuous lines correspond to periodic orbits in the vertical family around the displaced L_2 for a fixed value of β. Here we show the results for $\beta = 0, 0.01, 0.02, 0.03$ and 0.04. On the other hand, the points in the dashed lines correspond to periodic orbits with a fixed orbital period $T = 3\pi/2, \pi, 2\pi/3$ (i.e. 9, 6 and 4 months respectively). We note that each orbit in the discontinuous lines has a different value for the sail lightness number β.

All the orbits presented here are linearly unstable; this means that an active control must be applied to remain close to the orbit. Nevertheless, we find two classes of linear dynamics around the periodic orbits: saddle $\times$ centre orbits (blue lines) and saddle $\times$ saddle orbits (red lines). This affects to the behaviour of the trajectories followed by a solar sail close to a periodic orbit. In both cases the trajectories will quickly escape from a small vicinity orbit due to their instability. Close to a saddle $\times$ centre orbit, the trajectory will escape along the unstable direction given by the saddle. Instead, for a saddle $\times$ saddle orbit, there are two expanding directions, each one related to a saddle plane. In many cases, one of the two expanding directions is stronger than the other one, and the trajectories will escape along the strongest direction. But when the instability of the two saddles is comparable in terms of "strength", we will have a 2D family of escaping directions. In this case, keeping the trajectory of a solar sail close to a reference orbit can be harder, as there are more possible escape trajectories. We recall that the "strength" of the instability is related to the modulus of the real positive eigenvalues.

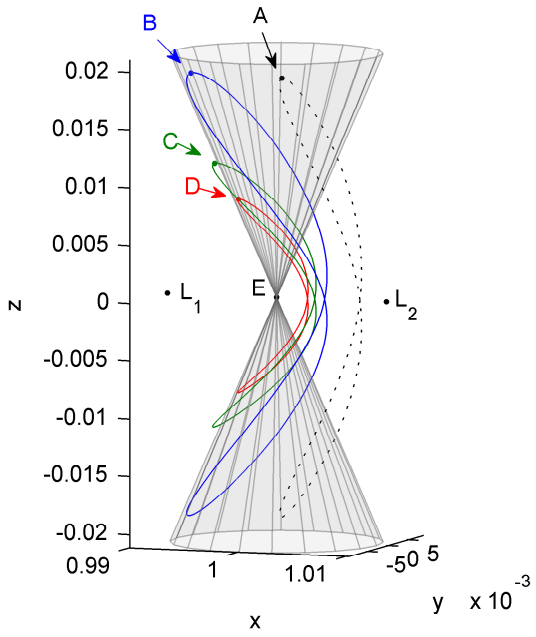

Fig. 3: Four orbits in the Vertical Lyapunov family around L_2 that present favourable visibility properties for a Polar mission.

Table 1: Characteristics of the considered orbits.

Id	β	T	X_0	Z_0	$V_{Y,0}$
A	0	$\frac{3}{2}\pi$	1.00049	0.01897	0.00740
B	0.02	$\frac{3}{2}\pi$	0.99215	0.01912	0.01200
C	0.026	π	0.99432	0.01138	0.01057
D	0.04	$\frac{2}{3}\pi$	0.99650	0.00837	0.00790

In the work by Ceriotti and McInnes[7] four orbits were identified, due to their favourable visibility properties, as well as period (sub-multiple of the year) and lightness number. They are symmetric with respect to the ecliptic plane, and therefore offer the same coverage of both poles. The orbits were identified with the letters from A to D. These orbits are plotted in Figure 3, and their main characteristics are shown in Table 1, where T is the period of the orbit (in non-dimensional time units, i.e. 2π is 1 year), and $X_0, Y_0, V_{Y,0}$ are the non-null components of the initial state. Orbit A does not use a solar sail, and therefore a propulsion system must be used for its station keeping. For this reason,

the control of this orbit is beyond the scope of this paper. Instead, the other three orbits – B, C, D – will be used throughout the rest of this work.

IV. STATION KEEPING

As mentioned in the previous section, all the presented orbits are unstable, i.e. an arbitrary small perturbation in the state leads to an exponential divergence from the nominal orbit. Therefore, these orbits cannot be used for a relatively long interval of time unless an active control is used to keep the spacecraft close to the nominal orbit. In the following two subsections will investigate two different control strategies for this purpose. In section IV.I we propose a control strategy using a linear quadratic regulator and in section IV.II we use a control scheme based on the Floquet modes. We also test the performance of both methods to control a solar sail around orbits B, C and D described in the previous section.

IV.I Control Strategy using LQR

The control loop used here is based on a linear quadratic regulator (LQR),[8] applied in a similar way as in Ceriotti et al.[10]

As actuator for the control loop, we use the solar sail, assuming that we can steer it in the two directions, and also that its lightness number β can vary (within some limits). Therefore there are three control variables.

Steering a solar sail is a standard control method, which has been investigated in the literature extensively. In addition to the actuators commonly used on conventional spacecraft (inertia wheels, thrusters), sail steering can also be achieved exploiting the sail itself. Several methods were proposed, including shifting of the centre of mass with respect to the centre of pressure through moving masses,[11] deployment of control vanes at the edge of the sail,[12] and also differential change of reflectivity on opposite sides of the sail through photo-chromic areas.[13] These areas are covered with a special material that can change its reflectivity coefficient within a given range according to a current that is applied to it.

To avoid singularities that can arise due to the use of angles, the sail attitude is described here through Cartesian components of the vector $\hat{\mathbf{n}}$. We consider the following reference frame:

$$\begin{aligned} \hat{\mathbf{r}}_\mathbf{S} &\equiv \frac{\mathbf{r_S}}{r_S} \\ \hat{\theta} &\equiv \frac{\hat{\mathbf{z}}\times\hat{\mathbf{r}}_\mathbf{S}}{|\hat{\mathbf{z}}\times\hat{\mathbf{r}}_\mathbf{S}|} \\ \hat{\varphi} &\equiv \hat{\mathbf{z}}\times\hat{\theta} \end{aligned} \tag{2}$$

and consider that in this frame, the sail normal is $\hat{\mathbf{n}} = \begin{bmatrix} n_{r_s} & n_\theta & n_\varphi \end{bmatrix}^T$. Since $\hat{\mathbf{n}}$ is a unit vector, the second and third components are sufficient to reconstruct the whole vector, as:

$$n_{r_s} = \sqrt{1-(n_\theta^2+n_\varphi^2)} \tag{3}$$

where the sign is always positive, due to the sail pointing away from the sun and therefore $n_{r_s} > 0$.

We also neglect any delay in the response of the actuator, i.e. we assume that the sail normal can instantly point in any direction, as if the sail has null moments of inertia. This assumption is not completely unreasonable, provided that the motion of the spacecraft along the orbit is relatively slow (and therefore fast steering manoeuvres are not necessary), and also that only small corrections in the sail attitude are required (and so the slew manoeuvres can be quick).

The change of lightness number is basically a way to throttle the magnitude of the force provided by the sail, without changing its direction. Strictly speaking, considering the definition of the lightness number, and since the mass of the spacecraft is constant, β can only be changed by modifying the sail area. This can be achieved for example through the use of the same reflecting control vanes used for attitude control, but they would be deployed symmetrically, such that the centre of pressure is not shifted. However, another method is possible. The area of the sail that appears in the definition of β is in fact the reflective area. This can be reduced by, for example, temporarily making some portions of the sail (partially) non-reflective, again using the photo-chromic materials mentioned before. To be able to increase the lightness number with respect to the reference, the sail area shall be slightly bigger than the reference value, and part of it covered with opaque material that can then become transparent when needed.

A control vector can therefore be defined as:

$$\mathbf{u} = [n_\theta, n_\varphi, \beta] \tag{4}$$

For defining the control strategy, it is convenient to rewrite the equations of motion (1) as a first-order differential system, introducing the state vector $\mathbf{s} = [X, Y, Z, V_X, V_Y, V_Z]^T$:

$$\dot{\mathbf{s}}(t) = \mathbf{f}(\mathbf{s}, t) \tag{5}$$

Let us assume, at a given instant of time $\bar{t}$, that the spacecraft is at state $\mathbf{s}(\bar{t})$. At the same time, the reference state and control are $\mathbf{s_r}, \mathbf{u_r}$ respectively. The reference state defines the reference orbit as function of time, as discussed in the previous section. The reference control, along one orbit, is constant. In an ideal condition, the real state coincides with the reference one. However, due to the instability of the trajectory, in general the real state may differ from the reference one, and therefore the state error can be defined as: $\delta\mathbf{s} = \mathbf{s} - \mathbf{s_r}$. The objective of the controller is to find the additional component of control, $\delta\mathbf{u}$ (defined as the feedback control) such that the total control $\mathbf{u} = \mathbf{u_r} + \delta\mathbf{u}$ brings the spacecraft states back to the reference states after some time.

To compute $\delta\mathbf{u}$ at each instant of time, we use here a linear time-invariant approximation of the dynamical system. Due to this approximation, the real state shall be in the vicinity of the reference state. Furthermore, if we assume that the dynamics of the reference trajectory is slow enough, then we can approximate the time varying problem as a sequence of time-invariant problems, and use classic linear feedback control theory for computing the gain matrix. However, the optimal control problem shall be solved at each instant of time, and the gain matrix updated, as described in the following. For the specific control problem under consideration, the control vector $\mathbf{u}_{3\times1}$ contains two parameters for the attitude of the sail, and the third component is the lightness number of the sail itself.

The linearisation is done in the following way:

$$\mathbf{A}_{6\times6} = \left.\frac{\partial\mathbf{f}}{\partial\mathbf{s}}\right|_{\mathbf{s_r},\mathbf{u_r}} ; \ \mathbf{B}_{6\times3} = \left.\frac{\partial\mathbf{f}}{\partial\mathbf{u}}\right|_{\mathbf{s_r},\mathbf{u_r}} \tag{6}$$

where the function $\mathbf{f}$ represents the flow reduced to a first-order differential system of six equations, according to Eq. (5). The derivatives of $\mathbf{f}$ with respect to states $\mathbf{A}$ and controls $\mathbf{B}$ are found analytically (their expression is omitted here), and then evaluated numerically. The dynamics of the system in the vicinity of $\mathbf{s_r}$, $\mathbf{u_r}$ can then be expressed as:

$$\delta\dot{\mathbf{s}} = \mathbf{A}\delta\mathbf{s} + \mathbf{B}\delta\mathbf{u} \tag{7}$$

This linear, time-invariant system approximates the real system at a given time and in the vicinity of the reference states and controls. It can be verified through the controllability matrix that the system in Eq. (7) is controllable. However, non-linearities, as well as bounds on the controls, will limit the applicability of this method to some maximum displacement from the reference. The problem is now to find the optimal feedback control history $\delta\mathbf{u}(t)$ for any time $t > \bar{t}$ such that the (linear) system of Eq. (7) will settle to the reference state, i.e. $\delta\mathbf{s} = 0$. We introduce the following cost function:

$$J(\delta\mathbf{u}) = \int_0^\infty \left(\delta\mathbf{s}^T\mathbf{Q}\delta\mathbf{s} + \delta\mathbf{u}^T\mathbf{R}\delta\mathbf{u}\right) dt \tag{8}$$

which aims at minimising the state error and the feedback control over an infinite amount of time, constrained to the linear flow in Eq. (7). The matrices $\mathbf{Q}, \mathbf{R}$ are weights that quantify the relative cost of each state and control in the cost function. For this problem, considering the normalisation of the variables introduced in the CR3BP, the following weights were used:

$$\begin{array}{l}\mathbf{Q} = \text{diag}\left(\begin{bmatrix}10 & 10 & 10 & 1 & 1 & 1\end{bmatrix}\right) \\ \mathbf{R} = \text{diag}\left(\begin{bmatrix}10^{-4} & 10^{-4} & 10^{-1}\end{bmatrix}\right)\end{array} \tag{9}$$

The choice of these coefficients was done initially following Bryson's rule ($\mathbf{Q}$, $\mathbf{R}$ diagonal with Q_{ii} = maximum acceptable value of δs_i^2, R_{ii} = maximum acceptable value of u_i^2), and then adjusted with a heuristic procedure.

We now assume a control proportional to the state error, $\delta\mathbf{u} = -\mathbf{K}\delta\mathbf{s}$. Minimising Eq. (8) under this assumption leads to the well-known algebraic Riccati equation,[8] which can be solved analytically to compute the gain matrix $\mathbf{K}_{3\times6}$.

The total control can then be computed, and saturation is applied, to enforce the maximum deflection of the sail with respect to the Sun direction, and the maximum variation in lightness number. The following intervals are considered for each control variable:

$$\begin{array}{l}n_\theta, n_\varphi : [-1, +1] \\ \beta : [\beta_r - 0.002, \beta_r + 0.002]\end{array} \tag{10}$$

If a control variable is out of its interval, then it is set equal to the closest bound. However, this is not sufficient to guarantee a real solution for Eq. (3), so additionally, if $\sqrt{n_\theta^2 + n_\varphi^2} > 1$, then the two components are rescaled dividing both of them by $\sqrt{n_\theta^2 + n_\varphi^2}$.

The resulting control is then fed into the integration of the flow. At the next time step in the integration, the procedure is restarted to update the feedback control.

IV.I.I Results

This control method was implemented in MATLAB/Simulink and applied to the orbits B, C, D. In the following we will show, through test-cases, that not only is the controller able to stabilise the non-linear system, but also that it is able to bring the spacecraft back to the reference states, when the initial state is perturbed. This can be interpreted as the step response of the controlled system, when the step is applied at time $t = 0$, and therefore at the northern apex of the orbits. The following plots represent, for each orbit, the results of the controlled system. For orbit B, the controller can cope with initial displacements of order 10^{-4} (about 15,000 km) in each position component and 10^{-3} (about 30 m/s) in each velocity component simultaneously. For greater displacements, the spacecraft diverges indefinitely from the reference.

Figure 4 shows the reference trajectory, and the trajectory followed when this initial displacement is applied to the states, for both the controlled and the uncontrolled system (i.e. keeping sail attitude and lightness number fixed to reference values). It can be seen that the controlled system winds onto the reference, while the uncontrolled system quickly diverges from it within a fraction of the orbital period. Figure 5 shows the state error $\delta\mathbf{s}$ (split into position and velocity components): it is clear that the system reaches the reference conditions (null error) within less than one orbital period. The control effort required is shown in Figure 6. Instead of plotting the components of $\hat{\mathbf{n}}$, which are used as control variables, the angular sail displacement with respect to the reference is shown. Despite this (scalar) angle does not fully characterise the attitude of the sail, it can be used as a measure of the slew manoeuvre needed, and it is computed through $\arccos(\langle\hat{\mathbf{n}}, \hat{\mathbf{n}}_\mathbf{r}\rangle)$, where $\hat{\mathbf{n}}_\mathbf{r}$ is the reference attitude, i.e. pointing towards the x-axis.

Very similar results are obtained for orbit C, see Figures 7 and 8. The same maximum initial displacements can be controlled, and again the reference states are reached within one orbital period.

The control of orbit D, instead, is more difficult. With the same settings of the controller, the maximum initial displacements have to be halved with respect to orbits B and C (to 5×10^{-5} and 5×10^{-4}). At the same time, the system is not completely settled to the reference within the first period, as it can be seen from the figures, which are plotted for two orbital periods. Despite the required maximum sail tilt is about 20 deg, there is a sensible slew manoeuvre

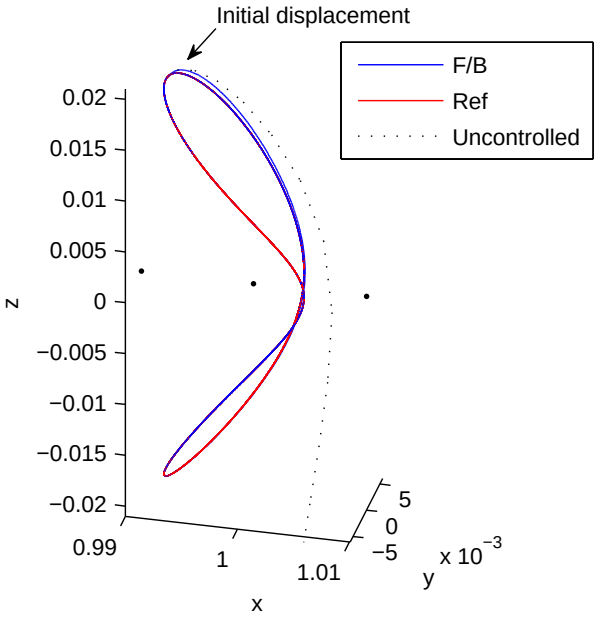

Fig. 4: Orbit B: reference (red), controlled trajectory (blue), uncontrolled trajectory (black, dotted).

changing the attitude of the sail rapidly, at $t = T/4$: this point corresponds to the spacecraft crossing the x-y plane. At this point, the velocity is highest, and this is also reflected in a rapid change in the velocity state error. The rapidly changing states at this point make the system difficult to control with an LQR, due to the approximation to a linear, time-invariant system.

To conclude this section, some final remarks that apply to all three cases. First, it can be seen that at the beginning of the simulation, when the state errors are high, the lightness number reaches its minimum allowed. Despite the linear controller loop would require a lower value of β, this cannot be provided as saturation is reached. A wider bound for β would certainly allow better control performance, in terms of convergence time and initial displacements allowed. However it can be difficult to implement in practice. Finally, it is worth noting that, given the initial displacement in position and velocity, the controller tries to quickly drag the velocity error down, but this results in a temporary increase in the position error. This is due to the tight interdependence between position and velocity in the non-linear flow.

IV.II Control Strategy using Floquet Modes (FM)

The control strategy used here is based on the ideas in previous works by Gómez et al.[9,14] for the station keep-

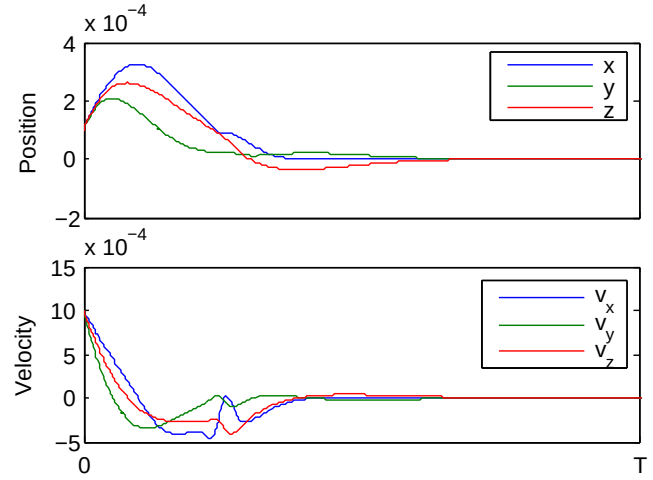

Fig. 5: Orbit B: state error with respect to reference trajectory.

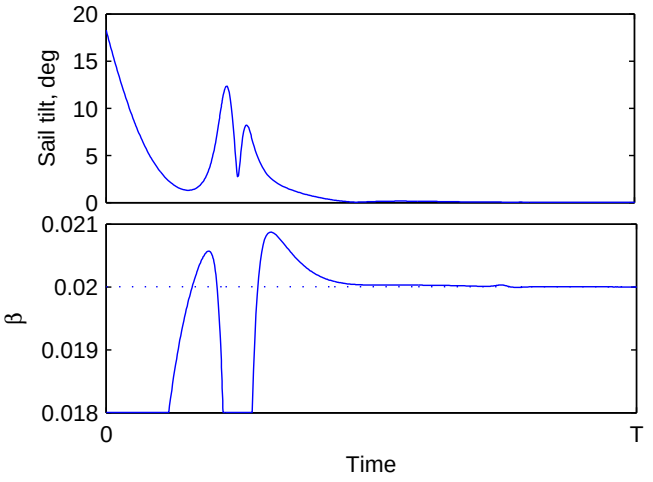

Fig. 6: Orbit B: control.

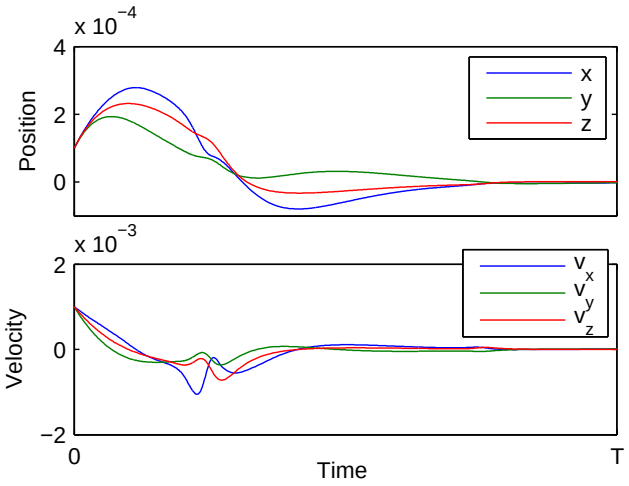

Fig. 7: Orbit C: state error with respect to reference trajectory.

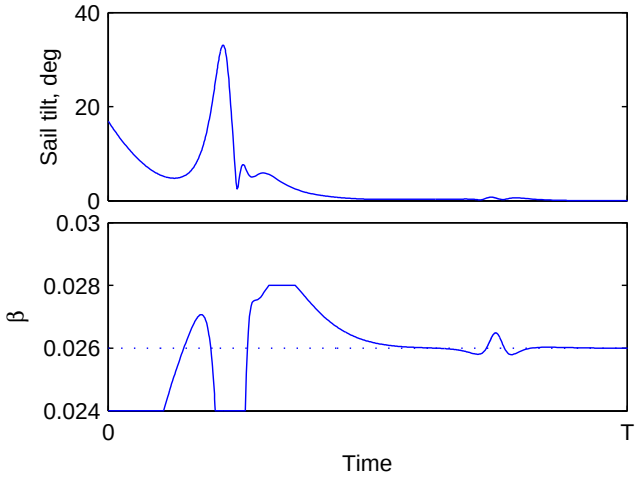

Fig. 8: Orbit B: control.

ing around a Halo orbits with a "traditional" thrust and by Farrés et al.[15,16] for the station keeping of a solar sail around an equilibrium point. This kind of strategies have already been tested successfully for the control of Halo orbits using a solar sail.[17]

For this control strategy we parameterise the sail orientation $\hat{\mathbf{n}}$ with two angles, α and δ, different from the ones described for the previous control. In the literature we find different definitions for these angles.[2,15,18] Here we define α as the angle between $\hat{\mathbf{n}}$ and the x-axis and δ the angle between $\hat{\mathbf{n}}$ and the ecliptic plane. Hence,

$$n_X = \cos\alpha\cos\delta,\ n_Y = \sin\alpha\cos\delta,\ n_Z = \sin\delta. \quad (11)$$

We note that all the periodic orbits found in Section III. have been found taking $\hat{\mathbf{n}} = (1,0,0)$, i.e. using this definition $\alpha_0 = \delta_0 = 0$.

The main differences between the strategy that we present here and the one described in section IV.I are: a) we only use two control parameters for the actuator, α and δ the two angles defining the sail orientation; and b) the parameters vary in a discrete way along time (by this we mean that the sail orientation is keep fixed for a certain amount of time Δt_1, then it changes to another fixed orientation for Δt_2 and successively). Moreover, the strategy presented here maintains the trajectory of the solar sail close to the nominal orbit at all time, but never reaches the reference orbit as in the previous control (see section IV.I). This should not be a problem as in most cases the main goal is usually to remain close to a reference orbit.

As in the previous control we also assume the the changes on the sail orientation are done instantly. As we will see these changes are small and the time between manoeuvres

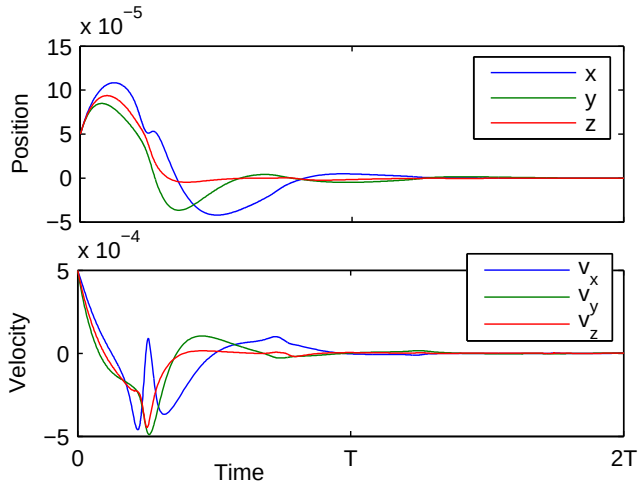

Fig. 9: Orbit D: state error with respect to reference trajectory.

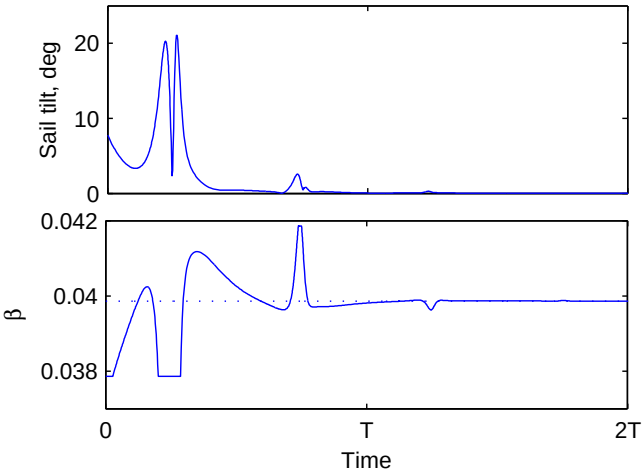

Fig. 10: Orbit D: control.

is long compared to the time it would take to change the sail orientation, hence it is a good approximation of the real case.

To derive a control law for the orientation of the solar sail we use information of the natural dynamics of the system around the reference periodic orbit. As we have seen in Section III. all the orbits in the vertical Lyapunov family described here are unstable. But there are orbits where the linear dynamics is centre $\times$ saddle and others where this one is saddle $\times$ saddle. The strategy to follow in each case is slightly different although in both cases we want to cancel out the instability given by the saddle(s).

In the case of centre $\times$ saddle orbits, when the sail is close to a reference orbit with the sail orientation fixed at $\alpha_0 = \delta_0 = 0$, the trajectory will escape along the unstable manifold. To control the instability given by the saddle we need to find a new sail orientation (α_1, δ_1) that brings the trajectory close to the stable manifold of the reference orbit. Then we can restore the sail orientation (α_0, δ_0) and let the dynamics act again. We can repeat this process over and over so that the trajectory remains close to the nominal orbit. Nevertheless, when we choose the new sail orientation we also need to take into account the projections of the trajectory in the other directions. In some cases changes on the sail orientation can result of an unbounded growth on the centre or neutral directions, experiencing a drift from the reference orbit and resulting with an escape trajectory. The same dynamics is found around Halo orbits for a solar sail.[17]

In the case of saddle $\times$ saddle orbits, the stable and unstable manifolds have larger dimensions, this can sometimes play in our favour. In many cases one of the two expanding directions will be much stronger than the other (specially close to bifurcation point in the family of periodic orbits). Hence the trajectory will escape faster along one of the two saddles and just focusing on the instability given by the strong saddle suffices. Nevertheless, in both cases the idea for the station keeping strategy is the same, at a certain point when the sail is escaping along the unstable manifold we change the sail orientation (α_1, δ_1) so that the trajectory comes close to the stable manifold, and we repeat this process over and over. As in the previous case, to decide the appropriate sail orientation we also need to take into account the neutral direction so that this one does not grow.

It is not obvious how to choose the appropriate new sail orientation so that the trajectory remains close to the reference orbit. First of all we need to track at all time the relative position between the sail's trajectory and the stable and unstable manifolds. We use the *Floquet Modes*, six T-periodic functions $\bar{\mathbf{e}}_\mathbf{i}(\tau)$, as a reference system around the reference periodic orbit. The main advantage of the Floquet modes is that the linear dynamics around the orbit is expressed in a simple way by considering the 3 planes generated by the couples $(\bar{\mathbf{e}}_{\mathbf{2i}}(\tau), \bar{\mathbf{e}}_{\mathbf{2i+1}}(\tau))$. The first plane is related to the linear approximation of the saddle (or the strongest saddle when we have two saddles). The second plane relates to the eigendirections with complex eigenvalues of modulus 1 and the dynamics on this plane is a rotation around the periodic orbit (or the remaining saddle when we have two saddles). The third plane will always be related to neutral eigenvalues, one of them will be the tangential direction to the orbit, and the other is along the variation of the family of periodic orbits. A drift of the trajectory in this third plane results on a drift along the family

of periodic orbits and must be avoided. For details on how to define the Floquet modes see the work by Gomez et al.[9]

Finally, to find the appropriate changes on the sail orientation we will use the information given by the first order variational flow. We recall that, if $\phi_{\Delta t}(t_0, x_0, \alpha_0, \delta_0)$ is the flow at time $t_1 = t_0 + \Delta t$ of the vector field in Eq. (1) starting at $t = t_0$ with $(x = x_0, \alpha = \alpha_0, \delta = \delta_0)$, then,

$$\begin{aligned} \mathcal{F}(\Delta t, \Delta\alpha, \Delta\delta) &= \phi_{\Delta t}(\chi_0) + \frac{\partial \phi_{\Delta t}}{\partial \alpha}(\chi_0) \cdot \Delta\alpha \\ &+ \frac{\partial \phi_{\Delta t}}{\partial \delta}(\chi_0) \cdot \Delta\delta. \end{aligned} \tag{12}$$

is the first order approximation of $\phi_{\Delta t}(t_0, x_0, \alpha_0 + \Delta\alpha, \delta_0 + \Delta\delta)$, where for $\chi_0 = (t_0, x_0, \alpha_0, \delta_0)$.

Notice that $\mathcal{F}(\Delta t, \Delta\alpha, \Delta\delta)$ is a linear application that given $(t_0, x_0, \alpha_0, \delta_0)$ gives us an approximation of the position of the trajectory at time $t = t_0 + \Delta t$ when a change $(\Delta\alpha, \Delta\delta)$ on the sail orientation has been applied at time $t = t_0$. This application will tell us what change $(\Delta\alpha, \Delta\delta)$ and for how long Δt we have to apply it to bring the sail's trajectory close to the reference orbit.

For the control strategy we define 3 parameters (ε_{max}, dt_{min} and dt_{max}) which depend on the mission requirements and the dynamics around the reference orbit ($N_0(t)$). Here: ε_{max} is the maximum distance to the stable direction allowed, used to decide when we have to change the sail orientation; and dt_{min}, dt_{max} are the minimum and maximum time allowed between manoeuvres.

To fix notation, if $\varphi(t_0)$ is the position and velocity of the solar sail at time t_0, then

$$\varphi(t_0) = N_0(t_0) + \sum_{i=1}^{6} s_i(t_0)\bar{\mathbf{e}}_\mathbf{i}(t_0),$$

where $N_0(t)$ is the reference periodic orbit we want to remain close and $\bar{\mathbf{e}}_\mathbf{i}(t)$ are the six Floquet modes.

When we are close to $N_0(t_0)$ we set the sail orientation $\alpha = 0, \delta = 0$. Due to the saddle(s) the trajectory will escape along the unstable direction(s). When $|s_1(t_1)| > \varepsilon_{max}$ (or $|s_3(t_1)| > \varepsilon_{max}$ in the case of two saddles), we consider that the sail is about to escape so we need to change the sail orientation. We use $\mathcal{F}(\Delta t, \Delta\alpha, \Delta\delta)$ to find the new sail orientation α_1, δ_1 and time $dt_1 \in [dt_{min}, dt_{max}]$ so that by changing the sail orientation at $t = t_1$, then at $t = t_1 + dt_1$ the sail trajectory is close to the stable manifold of the reference orbit. Finally, at $t_1 + dt_1$ we will restore the sail orientation to $\alpha = 0, \delta = 0$ and we repeat this process during the mission lifetime.

IV.II.I Finding α_1, δ_1 and dt_1

Let us briefly describe a way to find $\Delta\alpha_1, \Delta\delta_1$ and dt_1 so that the flow at time $t^* = t_1 + dt_1$ is close to the reference orbit. We recall that we want the trajectory to come close to the stable manifold, i.e. $s_1(t^*) = 0$ (and $s_3(t^*) = 0$ in the case of two saddles), and that the centre projection $(s_3(t^*), s_4(t^*))$ (when present) and the neutral direction $(s_5(t^*), s_6(t^*))$ do not grow. Essentially we want to find a new sail orientation α_1 and δ_1 such that after a finite time dt_1 the trajectory is inserted into the stable manifold so that then the trajectory naturally comes back to the reference orbit. This might not always be possible, but trajectories that come close to the stable manifold are also good for our purpose.

To find α_1, δ_1 and dt_1 we proceed as follows: We take different times $\tilde{t}_i$ for $i = 0, \ldots, n$, with $t_i \in [t_1 + dt_{min}, t_1 + dt_{max}]$ defined as $\tilde{t}_i = t_1 + dt_{min} + i \cdot dt$ and $dt = (dt_{max} - dt_{min})/n$, and for each $\tilde{t}_i$ we compute the variational map $\mathcal{F}(i \cdot dt, \Delta\alpha, \Delta\delta)$.

(a) If the orbit is centre $\times$ saddle, for each $\tilde{t}_i$ we find $\Delta\alpha_i, \Delta\delta_i$ such that, $s_1(\tilde{t}_i) = s_3(\tilde{t}_i) = s_4(\tilde{t}_i) = 0$.

Note that this reduces to solve a linear system with 2 unknowns and 3 equations, which we solve using the least square method.

(b) If the orbit is saddle $\times$ saddle, for each $\tilde{t}_i$ we find $\Delta\alpha_i, \Delta\delta_i$ such that, $s_1(\tilde{t}_i) = s_2(\tilde{t}_i) = 0$.

Note that this reduces to solve a linear system with 2 unknowns and 2 equations, which can be solved exactly in the non-degenerate case.

Now we have a set of $\{\tilde{t}_i, \Delta\alpha_i, \Delta\delta_i\}_{i=1,\ldots,n}$ found in the previous step. We choose $\tilde{t}_j, \Delta\alpha_j, \Delta\delta_j$ such that $||(s_5(\tilde{t}_j), s_6(\tilde{t}_j))||$ is the smallest (i.e. the divergence in the neutral direction is as small as possible).

Hence, the parameters that will bring the sail back to the nominal orbit are:

$$\alpha_1 = \Delta\alpha_j, \quad \delta_1 = \delta_0 + \Delta\delta_j, \quad dt_1 = \tilde{t}_j - t_1. \tag{13}$$

IV.II.II Results

This control method has been implemented in ANSI C and applied to the orbits B, C, D described in Section III.. The linear dynamics for orbits B and C is saddle $\times$ saddle and orbit D is centre $\times$ saddle. So the algorithm for choosing α_1, δ_1 and dt_1 will be different according to the kind of

orbits. For each orbit we have applied the station keeping strategy during 10 orbital revolutions managing to maintain the solar sail trajectory close to the nominal reference orbit. For all three orbits we have used the same control parameters $\varepsilon_{max} = 10^{-5}$ AU (≈ 1495.98 km), $dt_{min} = 30$ days and $dt_{max} = 115$ days.

Figure 11 shows the trajectory that the spacecraft follows when the station keeping is applied for 10 orbital revolutions for orbit B, as we can see it remains close to the reference orbit. In Figure 12 we plot the error in position and velocity along time, where the error is computed as the difference between the reference orbit and the path followed by the solar sail. Finally, in Figure 13 we show the variations on the sail orientation (α, δ) through time. We recall that these changes are instantaneous.

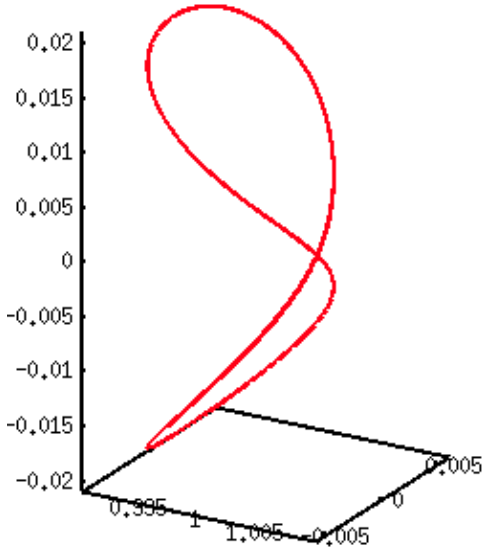

Fig. 11: Orbit B: controlled trajectory.

Figures 14 and 15 present the results for the control applied to orbit C, the errors on position and velocity along time and the variation of the sail orientation respectively. Similarly, Figures 16 and 17 display the results for orbit D after the control has been applied.

Notice that for all three orbits the trajectory remains bounded thought out the 10 orbital periods. In Figures 12, 14 and 16 we see that how the errors in position and velocity oscillates along time but never exceeds $5 \cdot 10^{-5}$ for the error in position and $8 \cdot 10^{-5}$ for the error in velocity.

To better understand how the changes the sail orientation affect the trajectory of the solar sail and this one is forced to come back to the reference orbit, we should have to look at the projection of the trajectory in the Floquet modes reference frame $\bar{\mathbf{e}}_\mathbf{i}$. There we would see how for orbits B and

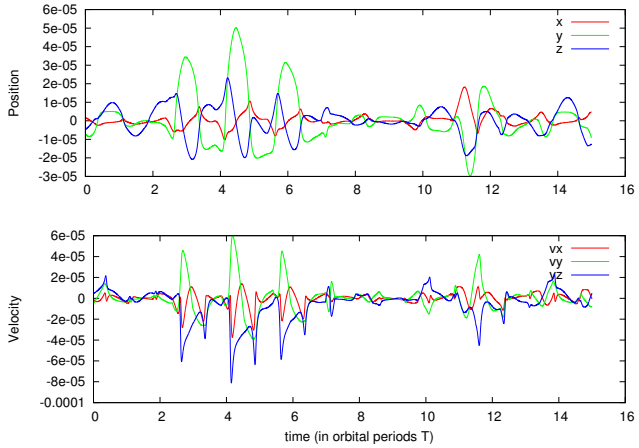

Fig. 12: Orbit B: state error with respect to reference trajectory in AU.

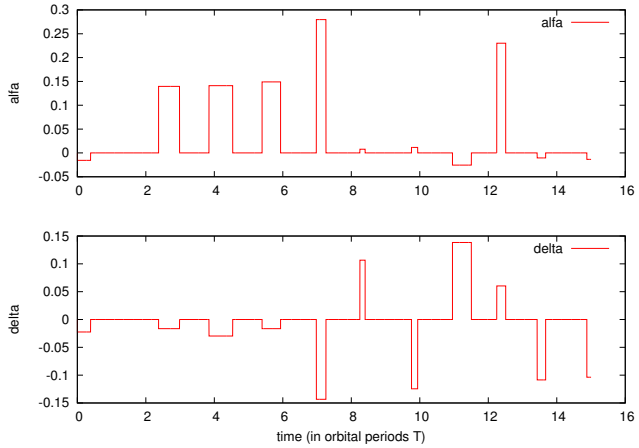

Fig. 13: Orbit B: control; variation in degrees of the sail orientation α (top) and δ (bottom).

C, the trajectory in the two saddle planes, changes on the sail orientation make the trajectory come close to the stable manifold (i.e. $s_1(t^*), s_3(t^*) \approx 0$). And for orbit D, the trajectory on the saddle plane shows the same behaviours as for orbits B and C, while in the centre projection the trajectory is a sequence of rotations that remains bounded though time. For all three orbits the dynamics in the neutral plane $(\bar{\mathbf{e}}_\mathbf{5}, \mathbf{ebar_6})$ also remains bounded.

If we look at the changes on the sail orientation, Figures 13, 15 and 17 we can see that these ones are discrete in time and they are small (less than 1° in most of the cases). We must mention that in this kind of strategies there is a strict relation between how close you want to remain from the reference orbit (ε_{max}) and amplitude of the variations on the sail orientation.

By choosing a larger value for ε_{max} we would then have

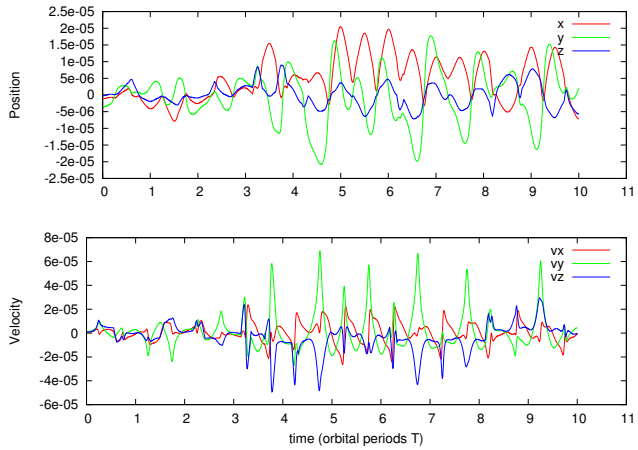

Fig. 14: Orbit C: state error with respect to reference trajectory in AU.

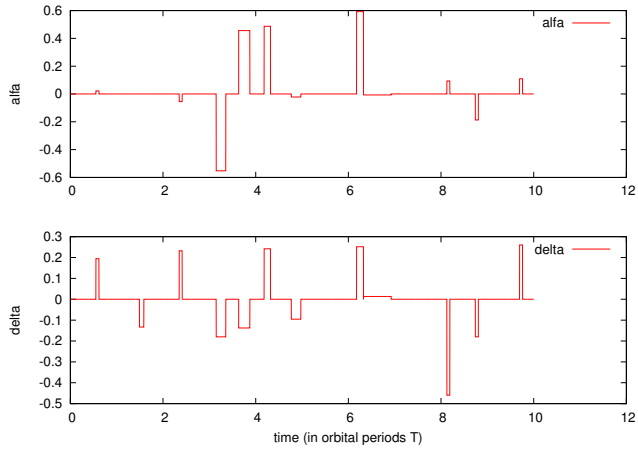

Fig. 15: Orbit C: control; variation in degrees of the sail orientation α (top) and δ (bottom).

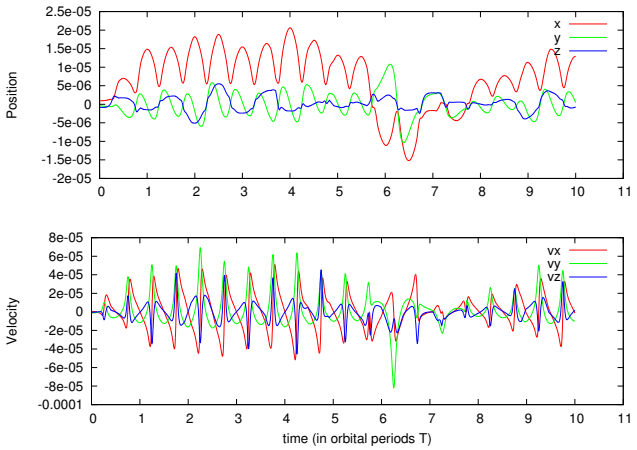

Fig. 16: Orbit D: state error with respect to reference trajectory in AU.

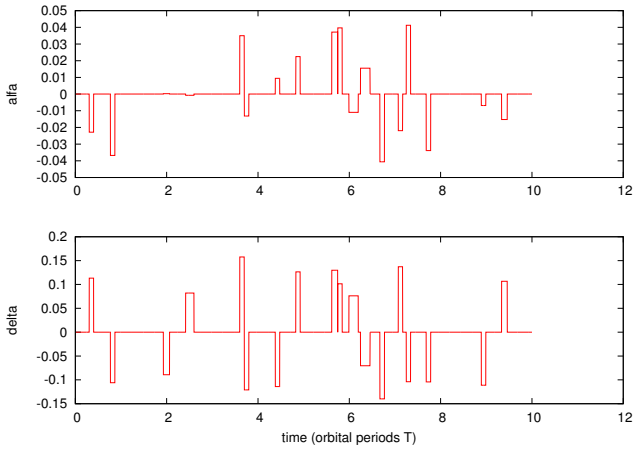

Fig. 17: Orbit D: control; variation in degrees of the sail orientation α (top) and δ (bottom).

larger changes on the sail orientation. But, due to the fact that we only use the information given by the linear dynamics of the system to make decisions, in some cases we would not be able to control the trajectory. Preliminary studies show that only for orbit B we could deal with larger displacements and hence larger changes on the sail orientation.

V. CONCLUSIONS

The paper presented a preliminary study on the controllability of the displaced vertical Lyapunov orbits with solar sails. Two control strategies were studied: a linear quadratic regulator (LQR) and a strategy based on Floquet modes (FM).

Both strategies were able to control the orbits. The FM are able to control the system by only varying the sail attitude. Instead, the LQR requires also β as a control parameter, although the required variation is small. If β were not included in the control vector the trajectory would diverge.

Moreover, it resulted that the FM uses extremely small changes in attitude to control the system, which is definitely a good point. However, these manoeuvres are instantaneous. Conversely, the LQR requires much bigger slew manoeuvres, but the control law is smooth in time.

The results also highlighted that LQR guarantees convergence with errors that are approximately one order of magnitude bigger than the FM, and this is related to the advantage of using an additional control parameter, as well as larger angular displacements of the sail.

An interesting remark is that for both strategies the convergence in the case of saddle $\times$ saddle orbits (orbits B

and C) is better than for the case the centre $\times$ saddle orbits (orbit D). This is probably due to the fact that for the former kind of orbits, the stable manifold is 3D while it is 2D for the latter. Hence there are more natural trajectories that asymptotically converge tot the reference orbit. Further studies must be done to confirm this fact.

A more extensive study on the relation between both strategies should be done, trying to relate in both cases the changes on the sail orientation with the dynamical properties of the system. This might help understand the differences between in the control between orbits B, C and D in the LQR case. Including the sail lightness number β as a control variable for the FM might also allow to consider larger variations on the sail orientation.

Finally, it would be interesting to study how both methods could be combined, to generate a more robust control scheme.

VI. ACKNOWLEDGEMENT

Ariadna Farres has been supported by the MEC grant MTM2009-09723 and the CIRIT grant 2009 SGR 67.

References

[1] Y. Tsuda, Osamu Mori, Ryu Funase, H. Sawada, T. Yamamoto, T. Saiki, T. Endo, and Jun'ichiro Kawaguchi. Flight status of ikaros deep space solar sail demonstrator. *Acta Astronautica*, 69:833–840, 2011. doi:10.1016/j.actaastro.2011.06.005.

[2] C.R. McInnes. *Solar Sailing: Technology, Dynamics and Mission Applications*. Springer-Praxis, 1999.

[3] C.R. McInnes, A.J.C. McDonald, J.F.L. Simmons, and E.W. MacDonald. Solar sail parking in restricted three-body system. *Journal of Guidance, Control and Dynamics*, 17(2):399–406, 1994.

[4] Colin Robert McInnes. The existence and stability of families of displaced two-body orbits. *Celestial Mechanics and Dynamical Astronomy*, 67(2):167–180, 1997.

[5] T.J. Waters and C.R. McInnes. Periodic orbits above the ecliptic plane in the solar sail restricted 3-body problem. *Journal of Guidance, Control and Dynamics*, 30(3):786–693, 2007.

[6] A. Farrés and À. Jorba. Periodic and quasi-periodic motions of a solar sail around the family SL_1 on the Sun - Earth system. *Celestial Mechanics and Dynamical Astronomy*, 107:233–253, 2010.

[7] Matteo Ceriotti and Colin Robert McInnes. Natural and sail-displaced doubly-symmetric lagrange point orbits for polar coverage. *Celestial Mechanics and Dynamical Astronomy*, 2012. in press, doi:10.1007/s10569-012-9422-2.

[8] Arthur E. Bryson and Yu-Chi Ho. *Applied optimal control: optimization, estimation, and control (Revised printing)*. Taylor & Francis Group, New York, 1975.

[9] G. Gómez, J. Llibre, R. Martínez, and C. Simó. *Dynamics and Mission Design Near Libration Points - Volume I: Fundamentals: The Case of Collinear Libration Points*, volume 2 of *World Scientific Monograph Series in Mathematics*. World Scientific, 2001.

[10] Matteo Ceriotti and Colin Robert McInnes. Hybrid solar sail and solar electric propulsion for novel earth observation missions. *Acta Astronautica*, 69(9-10):809–821, 2011. doi:10.1016/j.actaastro.2011.06.007.

[11] Vaios J. Lappas, Stephen Wokes, Manfred Leipold, and Peter Falkner. Attitude control design for solar sail missions. In *6th International ESA Conference on Guidance, Navigation and Control Systems*, European Space Agency, (Special Publication) ESA SP, pages 191–194. European Space Agency, 2005.

[12] B. Wie. Solar sail attitude control and dynamics, part 1. *Journal of Guidance, Control and Dynamics*, 27(4):526–535, July-August 2004.

[13] Ryu Funase, Osamu Mori, Yuichi Tsuda, Yoji Shirasawa, Takanao Saiki, Yuya Mimasu, and Junichiro Kawaguchi. Attitude control of ikaros solar sail spacecraft and its flight results. In *61st International Astronautical Congress (IAC 2010)*. IAF, 2010.

[14] C. Simó, G. Gómez, J. Llibre, R. Martinez, and J. Rodriguez. On the optimal station keeping control of halo orbits. *Acta Astronautica*, 15:391–397, 1987.

[15] A. Farrés and Á. Jorba. Dynamical system approach for the station keeping of a solar sail. *The Journal of Astronautical Science*, 58(2):199 – 230, April–June 2008.

[16] A. Farrés and À. Jorba. On the station keeping of a solar sail in the elliptic sun - earth system. *Advances in Space Research*, 48:1785–1796, 2011.

[17] A. Farrés and À. Jorba. Station keeping of a solar sail around a halo orbit. *Acta Astronautica*, 2012. in press, doi:10.1016/j.actaastro.2012.07.002.

[18] L. Rios-Reyes and D.J. Scheeres. Robust solar sail trajectory control for large pre-launch modelling errors. In *2005 AIAA Guidance, Navigation and Control Conference*, August 2005.